



# Radiation belt dynamics and the plasmasphere

W. R. Johnston<sup>1</sup>, P. C. Anderson<sup>1</sup>, J. Goldstein<sup>2</sup>, and T. P. O'Brien<sup>3</sup>

<sup>1</sup>W. B. Hanson Center for Space Sciences, University of Texas at Dallas, Richardson, TX <sup>2</sup>Space Science and Engineering Division, Southwest Research Institute, San Antonio, TX <sup>3</sup>The Aerospace Corporation, Chantilly, VA



## Abstract

During geomagnetic disturbances, the plasmapause and the outer radiation belt exhibit very dynamic behavior in terms of radial location and particle populations. These behaviors have been shown to be correlated as a result of wave-particle interactions contributing to outer radiation belt particle energization and loss. The limited temporal coverage of plasmapause observations to date limits their usefulness in constraining radiation belt models. We are producing a database of plasmapause locations based on DMSP RPA observations of the light ion trough, the ionospheric signature of the plasmapause. Initial results show good agreement with IMAGE EUV plasmapause observations, with differences between DMSP and IMAGE identifications tending to result from plasmaspheric structure, e.g., notches and plumes. The DMSP-derived plasmapause is found to correlate well with outer radiation belt dynamics, including variations in the L values of precipitating particle microbursts observed by SAMPEX.

## Plasmasphere-radiation belt interactions

The plasmasphere is dynamically influenced by magnetospheric and ionospheric electric fields. The evolution of the plasmapause (PP) during active times can significantly affect the outer radiation belt:

- Summers *et al.* [1998] argue that enhanced electromagnetic ion cyclotron (EMIC) waves within the plasmasphere tend to scatter trapped electrons into the loss cone, depleting radiation belt particles inside the PP. At the same time, outside the PP whistler-mode waves tend to energize trapped electrons (Fig. 1).
- Goldstein *et al.* [2005] found that the outer radiation belt responded to radial movement of the PP during disturbed times with a time lag of several days.

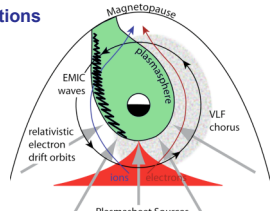


Fig. 1. Schematic of proposed mechanisms for outer radiation belt energization and loss associated with the plasmasphere. [From Reeves, 2007, after Summers *et al.*, 1998.]

## LIT and plasmapause

Ionospheric signatures of the PP include the light ion trough (LIT).

- Taylor and Walsh [1972] found the LIT one of the more consistent signatures.
- Foster *et al.* [1978] found the LIT equatorward a few degrees equatorward of the PP as identified by whistler waves.
- Grebowky *et al.* [1978] suggested supersonic upward H<sup>+</sup> flows result in LIT-plasmapause mismatch during refilling.

## Precipitating particle microbursts

Microbursts are short duration (<1 sec) bursts of relativistic electrons observed by low altitude satellites. They are believed to represent wave-particle scattering of energetic electrons into the loss cone, a side effect of whistler chorus energization of electrons outside the PP.

- Using SAMPEX data Nakamura *et al.* [2000] showed microbursts were associated with the dawnside and with post-storm recovery of the depleted radiation belt.
- Lorentzen *et al.* [2001a] showed innermost microburst locations during storms tended to track modeled PP location.
- Lorentzen *et al.* [2001b] linked microbursts to VLF chorus observed by Polar.
- O'Brien *et al.* [2003] linked microbursts to ULF activity at low L shells.

## Satellites/instrumentation: DMSP, IMAGE, SAMPEX

**DMSP:** polar sun-synchronous orbits, alt. 840 km, period 100 min., generally 3-4 operational at any given time. During 2001 data is available from F12, F14, and F15 in pre-midnight to morning and F13 in dusk to dawn.

**IMAGE:** eccentric polar orbit (from 1400 km alt. to 8 R<sub>E</sub>), operational 3/2000 to 12/2005. Instruments include:

- EUV imagers directly imaging 30.4 nm UV scattered by plasmaspheric He<sup>+</sup>. Such imaging is feasible when IMAGE is near apogee (Fig. 2).

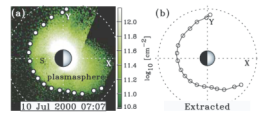


Fig. 2. Sample IMAGE EUV image of plasmasphere, showing extracted PP locations [from Goldstein *et al.*, 2004].

Instruments include:

- Retarding Potential Analyzer (RPA) providing ion density and composition
- Ion Drift Meter (IDM)
- Precipitating Electron and Ion Detectors (SSJ/4)

**SAMPEX:** low Earth orbit, operational 7/1992, altitude from 500 km to 620 km in 2001, includes four instruments for energetic particle measurements:

- Heavy Ion Large Area Proportional Counter Telescope (HILT)
- Low Energy Ion Composition Analyzer (LEICA)
- Mass Spectrometer Telescope (MAST)
- Proton/Electron Telescope (PET)

## Method and validation

Our approach uses the DMSP-observed LIT as identification of the low-altitude PP. The algorithm is illustrated in Fig. 3, with steps as follows (for free parameters, values used are in parenthesis):

- DMSP H<sup>+</sup> density data for MLAT 20°-65° (N or S), 4-sec sampling;
- smooth using Hanning window with fixed MLAT half width w (w=2°);
- reject passes where dynamic range of resulting series is less than β (β=10); also manually reject some passes (e.g. too noisy, no LIT visible on day side);
- identify all local minima in smoothed density;
- identify subset of these minima with a steep equatorward rise in density (density at least 3x greater 5° equatorward);
- proceed equatorward from each minima to location where density is higher than at minimum by factor f (f=1.3);
- manually identify one such location as plasmapause (may manually identify multiple boundaries in structured cases).

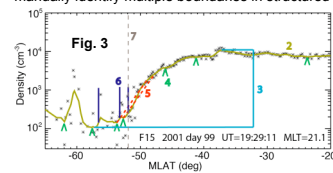
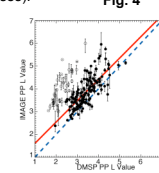


Fig. 4



For a 72-day period in 2001 (days 80-151), we obtained 2,392 PP identifications, an average of 33 per day (range of 3 to 63 per day). This represents 15% of the DMSP passes in this period; 34% of passes were rejected automatically and 50% were rejected manually. Most identifications were at dusk-midnight or predawn-dawn.

The PP locations in the ionosphere are mapped along magnetic field lines to the equatorial PP, using IGRF 2000 and Tsyganenko 2001 magnetic field models. Comparisons with SAMPEX may be done without external field mapping, since SAMPEX and DMSP are at similar altitudes.

Fig. 4 shows comparison of DMSP-identified PP L values to IMAGE identifications using a previous algorithm version described by Anderson *et al.* [2008]. Points ("error" bars) show average (range) of IMAGE-extracted PP locations within 15 min of time and 15 min of MLT of a DMSP identification. Comparisons form two clusters:

- Filled circles show main cluster (N=147, 79%) of good matches, with a mean L value difference of 0.45±0.43. Red line shows best fit for this cluster, blue dashed line represents identical L values.
- Open circles show second cluster of mismatches (N=40, 21%), with a mean L value difference of 1.78±0.45. Case-by-case examination of mismatches show that differences are often accounted for by highly structured plasmasphere conditions, including cases where DMSP is detecting plumes or notches.

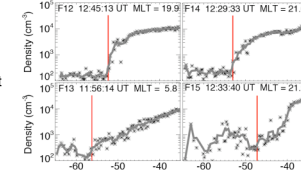


Fig. 5

Fig. 5 illustrates one such mismatch case:

- Left plots show DMSP H<sup>+</sup> observations with extracted PP (vertical red line), with three good matches and one mismatch (F15) within a 50 min. period
- Right plot shows DMSP mapped orbit tracks (red lines) and DMSP PP identifications (red asterisks) overlaid on an IMAGE observation projected onto the SM X-Y plane. The mismatch case maps to a plasmaspheric notch.

## Plasmapause, outer radiation belt, and microbursts

Results are shown for days 80-151 of 2001, the same period for which Goldstein *et al.* [2005] examined dynamic behavior of the PP and radiation belt:

- Fig. 6:
- Upper plot shows Dst.
  - Spectrogram shows SAMPEX observations of 1.5-6 MeV electron flux for L value vs. day (daily average of 0.1-L bins).
  - Heavy white line shows daily average PP location from DMSP (not separated by MLT); thin white lines show one standard deviation range in daily PP location.

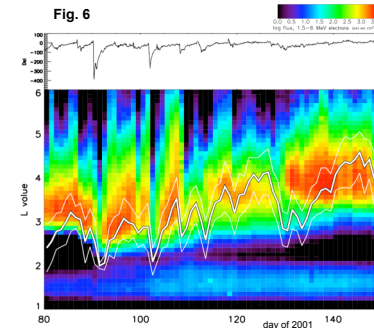


Fig. 7

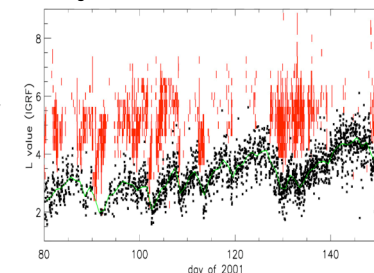


Fig. 8

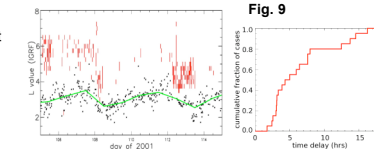
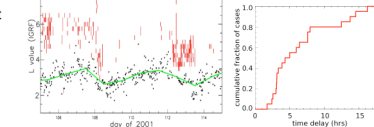


Fig. 9



Each storm/disturbance produces rapid plasmasphere erosion and depletion of the outer radiation belt (timescale ~1 day). Over following days the PP moves outward with refilling and the outer radiation belt is repopulated. If the PP overlaps the radiation belt, this may produce depletions of the radiation belt on timescales of days (e.g. after days 120 or 140).

- Fig. 7:
- DMSP-identified PP locations (black) with daily average (green).
  - Locations of SAMPEX-observed microbursts (red), by bins of 0.25 L within which one or more microbursts were detected.
  - Erosion-driven inward movement of plasmasphere is accompanied by prompt (timescale <1 day) inward movement of microburst locations, along with intensification.
  - Microbursts are consistently located outside of the PP, with isolated exceptions; this remains the case even on timescales less than a day.
  - During plasmasphere refilling, innermost microbursts tend to be ~0.5 L outward of outermost PP observations, suggesting a lower threshold in plasma density for microbursts than that for the DMSP-identified PP.

Fig. 8 is in the same format as Fig. 7, but shows days 105-115. On days 108 and 112, microbursts appear at L=4 within hours of the last PP detection at that L value.

During stormtime erosion at a given L shell, this time delay between last PP detection and first microburst detection provides some measure of the time scale for stormtime production of microbursts. Fig. 9 shows the cumulative fraction of observed cases (disturbance and L-shell) where this delay is less than or equal to a specified time. Observed microbursts increase at delays of ~3 hours.

## Conclusions and future work

- Our method of identifying the plasmapause using DMSP data compares well to IMAGE plasmapause observations; review of DMSP-IMAGE mismatch cases reveals that DMSP often observes plasmaspheric structure (e.g. notches, plumes) that account for mismatches.
- Comparison of locations for DMSP-identified plasmapause and SAMPEX-observed microbursts shows microbursts are consistently outside the plasmasphere, with correlations between locations of innermost microbursts and outermost plasmapause detections.
- During plasmasphere erosion, microburst locations move into emptied regions on short timescales; data suggests microbursts follow last plasmasphere detection by as little as ~3 hours.

This method is being applied to ~10 years of DMSP data, potentially providing ~100,000 plasmapause detections spanning a full solar cycle. Combined with SAMPEX data, the resulting database will be used to examine the relationship of the plasmasphere and radiation belt energization and loss.

## Acknowledgements

We gratefully acknowledge our data sources: the SAMPEX Data Center, ACE Data Center, NASA IMAGE mission, the Kyoto Data Center for Dst data, and the Center for Space Sciences at the University of Texas at Dallas and USAF for DMSP data. This work is supported by NASA NNX07AG39G and NASA grant NNX07AG39G.

## References

- Anderson, P. C., *et al.*, *GRL*, in press, 2008.
- Foster, J. C., *et al.*, *JGR*, 83:1175+, 1978.
- Goldstein, J., *et al.*, *GRL*, 31:L01801, 2004.
- Goldstein, J., *et al.*, *GRL*, 32:L15104, 2005.
- Grebowky, J. M., *et al.*, *Planet. Space Sci.*, 26:651+, 1978.
- Lorentzen, K. R., *et al.*, *GRL*, 28:2573+, 2001a.
- Lorentzen, K. R., *et al.*, *JGR*, 106(A4):6017+, 2001b.
- Nakamura, R., *et al.*, *JGR*, 105:15875+, 2000.
- O'Brien, T. P., *et al.*, *JGR*, 108(A8):1329+, 2003.
- Reeves, RBSP Science Overview, THEMIS presentation, 2007.
- Summers, D., *et al.*, *JGR*, 103(A9):20487+, 1998.
- Taylor, H. A., Jr., and W. J. Walsh, *JGR*, 77:6716+, 1972.

For further information: bobjohnston@utdallas.edu